

field of initial state variables was generated by imposing gravity, and so that void ratios known from boreholes were reproduced. Comparative calculations reveal that size and order of excavation steps had almost no influence on the displacements at the end of and after the excavation (b). The displacement paths of slope points are straighter in case of a fictitious simultaneous removal. Hook-shaped paths due to an excavation layer by layer were in fact observed via boreholes.

Karcher (2003) could also show by comparative calculations that plane strain may be assumed for unsupported trenches which are longer than twice their width. Observed horizontal displacements at the slope due to layer-wise excavation are shown in Fig. 12.4.7c. The good agreement with calculated values (d) is a validation as no parameters were adapted to get a fit. The calculated displacements exceed the actual ones as the observations started somewhat later than the excavation and were not continued after its end.

To *sum up*, excavation-induced evolutions of shape and state can be captured for a variety of ground and water conditions, but critical phenomena delimit the range of predictability. For psammoid ground with subcritical relative void ratio ($r_e < 1$) and slope inclination ($\beta < \varphi_{cs}$ in case of hydrostatic h_w) the displacement at the end of excavation is rather independent of its sequence and time. Cutting fine-grained saturated ground with $r_e > 1$ leads to a collapse. A steep slope ($\beta > \varphi_{cs}$) with gas channels can stand up to a height that can be estimated with the capillary skeleton pressure p_{cs} , but it collapses after drying or wetting. A cut exposing peloid to the air can collapse after a while if it is too steep and high. The gradual opening of cracks and disintegration into crumbs cannot yet be captured. The degradation of slopes cut into stiff fissured clay indicates that the combined diffusion of pore water and creep of skeleton can as yet only be estimated. Better predictions can be obtained with composite ground wherein narrow clay bands work as shear zones.

12.5 In-plane and anti-plane shaking

Boundary conditions for *in-plane shaking* are shown in Fig. 12.5.1. Nearly plane waves propagate through a package of horizontal layers in situ from a shaking base if fictitious lateral walls are suitably specified (a). The propagation would be one-dimensional (Sect. 11.4) if the time-dependent displacements for this case would be imposed to the walls. These displacements are not known in advance, they should be equal for opposite points of the two fictitious walls. This condition works also with inclined layers, then two thought walls are shifted downwards by repeated propagations (b). Velocity v_w and pressure p_w of the pore water are also the same at opposite wall points for this reduction to a one-dimensional problem. In particular, skeleton and pore water can undergo the same motion (no drainage), or the hydraulic height h_w can be independent of the skeleton motions (free drainage).

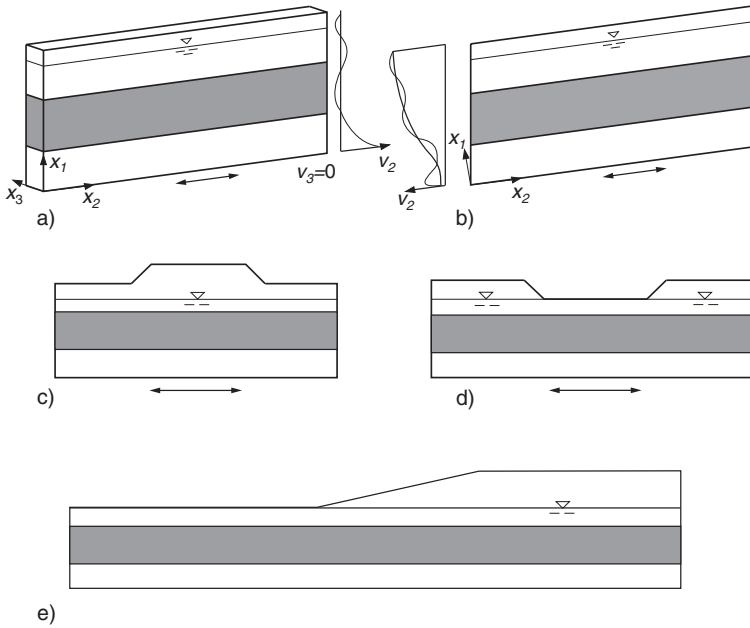


Fig. 12.5.1. Boundary conditions for in-plane shaking: free field with horizontal (a) and inclined layers (b), dam (c) and excavation (d) with layered ground, and different far-field levels (e)

If the ground has a more complex composition and/or an uneven surface conditions for fictitious boundaries cannot be justified as easily. With a symmetric dam (c) or trench (d) and parallel layers otherwise opposite points of walls undergo again the same displacements and have the same pressures. Beyond a sufficient distance from the symmetry line the far-field evolution is no more influenced by the dam or trench. A uniform shaking may be assumed at a sufficiently deep fictitious rigid base (cf. the beginning of Sect. 11.4). The symmetry of opposite walls gets lost with different ground levels on two sides of a slope (e). Evolutions around the slope may be captured by assuming a sufficiently deep rigid shaking base, and two walls with displacements and pore water conditions as for one-dimensional cases with the same ground profile. Comparative numerical calculations could show which distances suffice, analytical estimates are not in sight.

Different *shake boxes* have been used to investigate the range of validity. With rigid walls fixed to the base one-dimensional far-field propagations cannot be approached. This does not matter if the in-plane walls are well-defined and the plane-parallel walls are smooth. Thus the evolutions are plane-parallel and tractable enough for comparing observed and calculated evolutions, although they have no counterpart in situ. A set of laminar stiff frames can confine model soil upon a shaking base. Even if the frames are connected by stiff rods their mutual dislocations cause discontinuous boundary displacements of

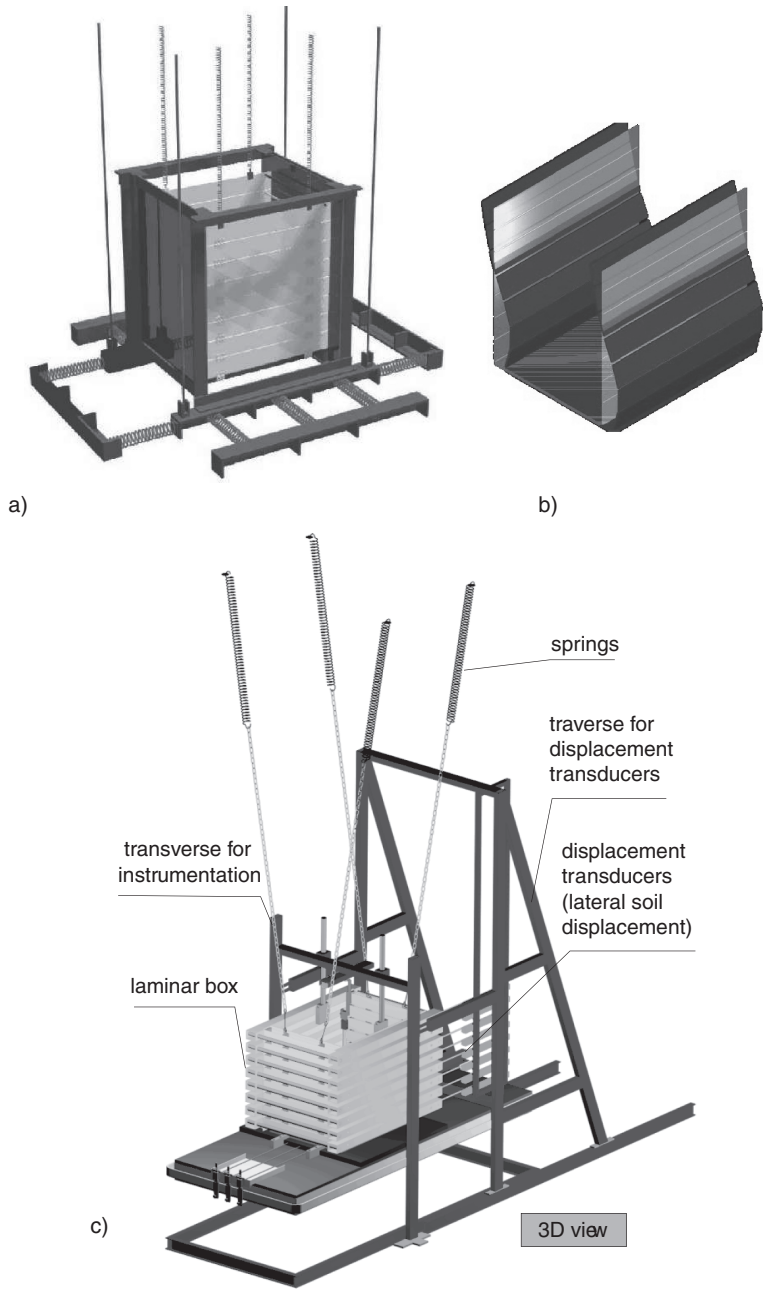


Fig. 12.5.2. Shake box with opposite laminate chains (**a**, **b** deformed), and with a jointed stack of frames (**c**); plots by Bühler (2006)

the soil. These may be smoothed by a membrane, but they lead to localizations which cannot be followed up in the analysis.

Prohibitive dislocations are avoided with *hinged laminar* lateral walls. In the first Karlsruhe shake box (Gudehus et al. 2004) the distance of opposite wall strips is fixed by wires, and the plane-parallel walls are smooth (Fig. 12.5.2a, b). The base is first clamped against springs and then released by cutting a wire. In the second one (Wienbroer et al. 2007) laminar frames with smooth flanks serve to the purpose (c). The base is shaken by a hydraulic drive with prescribed displacement vs. time, periodically or according to a seismic record. Vertical displacements along the in-plane walls are slightly confined by their friction. A membrane is needed between walls and saturated soil. An electro-phoretic water film can be employed instead for a peloid by means of direct current. These boundary conditions are sufficiently defined for back-analyses and resemble cases in situ.

Dry sand with a horizontal surface was investigated with the first Karlsruhe box, Fig. 12.5.3. It was loose at the onset and shaken by releasing the base. The free surface shifted sideways (a) and settled (b) rather uniformly. A back-analysis with hyp- δ (Libreros-Bertini 2006) reproduces this evolution in the essentials. As in the one-dimensional case (Fig. 12.4.2) the transversal waves have the same period as the base, whereas the longitudinal waves exhibit frequency doubling (later in the test and veiled by a shaking mode of the box).

Saturated sand was also tested in the first Karlsruhe box, Fig. 12.5.4. It was loose at the onset, its pore pressure p_w was measured near the base. Shortly after releasing the base the free surface was shifted (a) and settled (b), p_w rose abruptly and returned thereafter (c). The back-analysis with hyp- δ and no drainage in the first seconds reproduced the shift and the p_w -rise, but not the settlement afterwards and the p_w -reduction (Libreros-Bertini 2006). Pore water came out rapidly through spontaneously formed erosion channels (Sect. 8.4), this could be seen from minute volcanos (Sect. 16.3). Seepage is almost excluded in the short propagation time (Osinov 2000), the

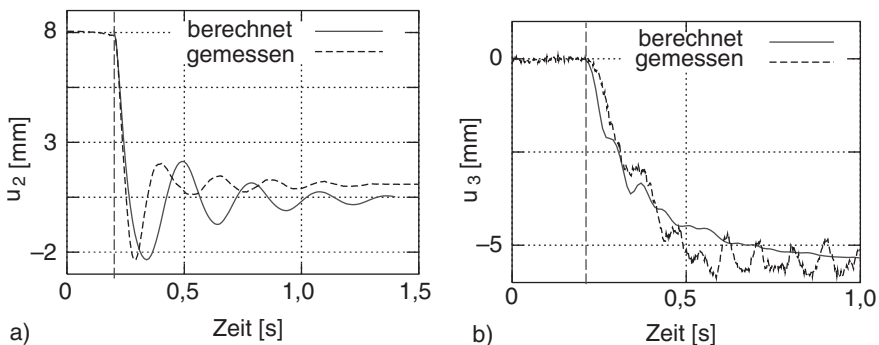


Fig. 12.5.3. Horizontal (a) and vertical (b) displacements of initially loose dry sand in the shake box of Fig. 12.5.2a and simulated with hyp- δ (Gudehus et al. 2004)

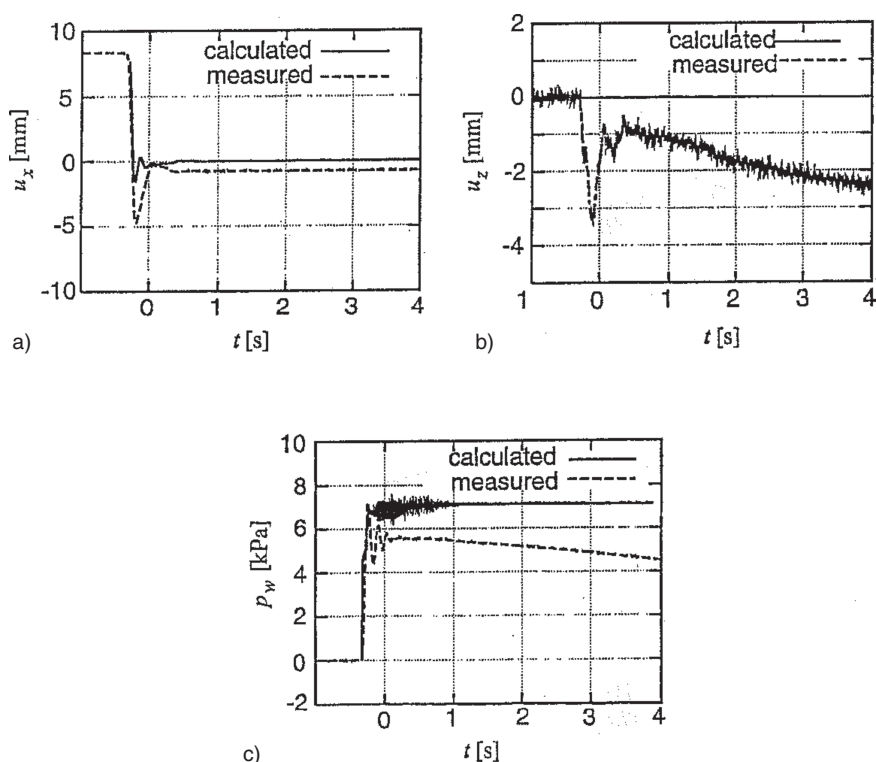


Fig. 12.5.4. Horizontal (a) and vertical displacements (b) and pore pressures (c), observed in the shake box of Fig. 12.5.2a with saturated loose sand and simulated with hyp- δ (Gudehus et al. 2004)

rapid dewatering via channels could not be captured by such a calculation (Kolymbas 1998).

The sand was densified to $e \approx e_d$ by repeated shaking and not shifted anymore. The same was achieved with periodic shaking in the second Karlsruhe box (Wienbroer et al. 2007). This attractor in the large could also be generated by hyp- δ with diffusion of pore water, except for hydrostatic uplift it depends on the amplitude as for a dry psammoid. With big enough amplitudes loose saturated sand expands to a suspension and exhibits gravity waves by strong shaking. The measured p_w reaches the total overburden pressure. This phenomenon and the subsequent formation of dewatering channels are outside the present reach (Sect. 16.3).

A layer of *saturated clay* upon a sand base was also investigated with the first Karlsruhe box. A moderately plastic clay was mixed and placed with a constant initial e so that a consolidation ratio $p_e/p_s \approx 1.5$ was attained near the sand base (Bühler 2006). Repeated shaking was imposed by stressing the box against springs with 1, 2, 4 and 8 mm stretching before release.

The observed response was almost the same in five repetitions, i.e. cumulative changes of state of the clay layer were rather negligible. The horizontal displacements along the wall increased slightly by doubling once and twice the base amplitude, but no more after a further doubling. This screening is confirmed by pore pressures p_w near the sand base. p_w rises slightly for a small amplitude, for a bigger one it reaches the total pressure and is reduced afterwards in some seconds.

These observations can be explained by means of v-hyp- δ . With moderate amplitudes the propagation of an S-wave in a peloid with $p_e/p_s < 1.5$ initially causes a slight reduction of p_s , after this increase of p_e/p_s the response gets nearly hypoelastic. With bigger amplitudes the underlying sand and the adjacent clay get temporarily close to a skeleton decay so that a further propagation is screened. A thin part of the clay layer is densified thereafter with pore water diffusion, this takes only a short time by (11.3.1). Further traces of propagations fade away by relaxation, thus the clay layer is the same as before except for a slight densification near the interface to the sand base. This near-attractor in the large would not occur with big amplitudes as then the clay would dilate in shear bands or crack, and could be transformed into a mud by strong shaking (Sect. 5.5).

Screening of shear waves is achieved by an about 1000 years old Japanese method named *hanshiku*. A mattress of fat clay with loose saturated sand inclusions was placed under important buildings. A strong earthquake causes a decay of the grain skeleton and only a minor subsequent densification, so the mattress which was kept wet served to the purpose repeatedly. Pralle (2002) observed a similar screening with a cushion of a saturated grain skeleton and a membrane (Fig. 12.5.5). The observed reduction of the top amplitude

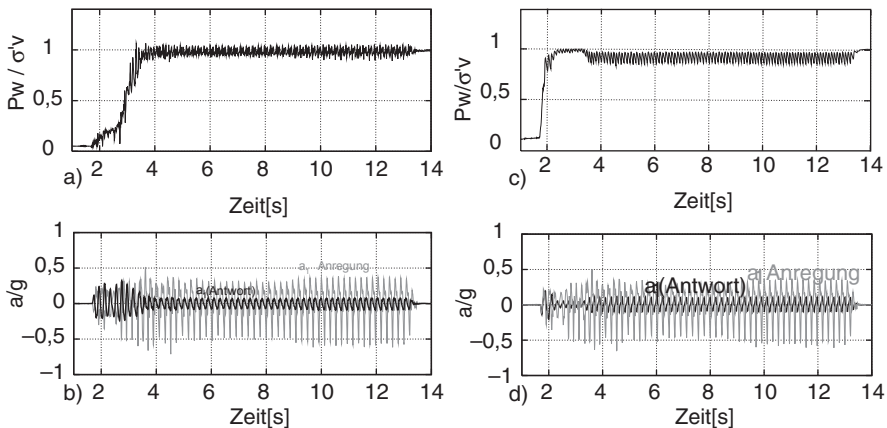


Fig. 12.5.5. Screening by skeleton decay: Pralle's (2002) observed pore pressure (a) and screening (b, inner line, outer zig-zag for excitation), simulation with hyp- δ (c and d) by Libreros-Bertini (2006)

(b) corresponds to the p_w -increase up to skeleton decay (a). Libreros-Bertini (2006) obtained nearly the same response by means of hyp- δ (c, d), this is a further validation.

Figure 12.5.6a shows a psammoid body including a *dam* under harmonic in-plane or anti-plane shaking (Gudehus et al. 2004, Libreros-Bertini 2006). In the latter case the out-of-plane displacements are equal in parallel cross sections, and the two fictitious walls are fixed and smooth. These boundaries are far enough from the dam, opposite wall points have the same displacements in case of in-plane shaking. Spreading (b) and settlement (c) of the dam calculated with hyp- δ , assuming $r_e = 0.5$ initially and no water, increase almost equally with time for both modes of shaking with amplitude $a_o = 0.2g$ and frequency $f = 3 \text{ s}^{-1}$. After a transition the displacement increases about

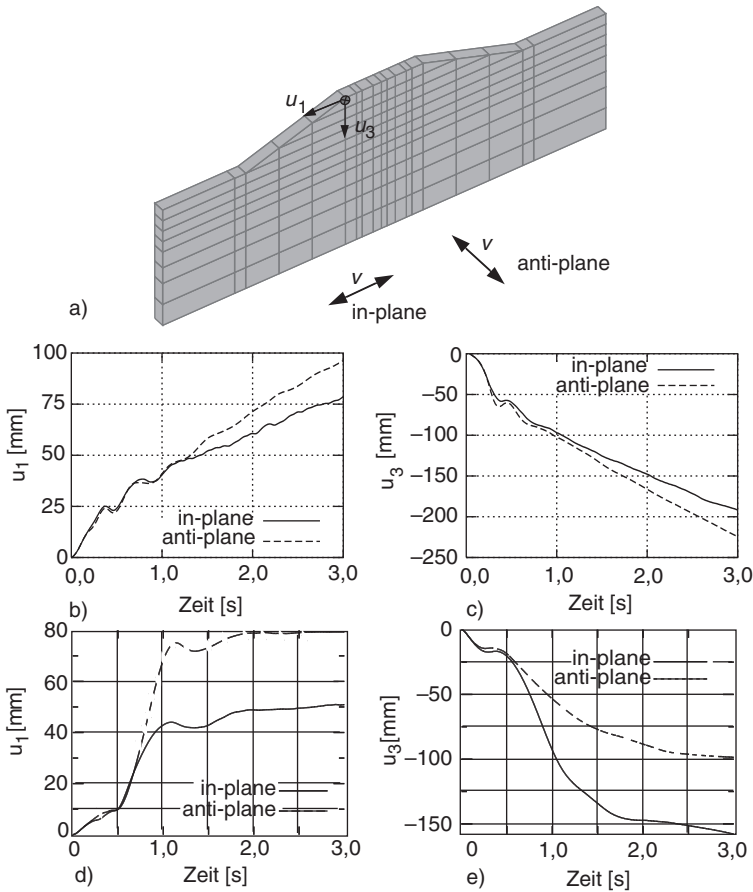


Fig. 12.5.6. Simulated seismic response of psammoid bodies with a dam (Gudehus et al. 2004, Libreros-Bertini 2006): boundary conditions (a), spreading (b) and settlement versus time without pore water (c), same with pore water (d, e)

linearly with the number of cycles, and the ratio of both components is rather constant. The latter is nearly independent of the frequency f , but the rate of growth per cycle is almost 20 times as big for $f = 2 \text{ s}^{-1}$ as for 15 s^{-1} . This magnification has little in common with the resonance of linearly elastic bodies.

The response of such a psammoid body was also calculated with water saturation and without drainage (Gudehus et al. 2004). The latter assumption is justified for some cycles with the assumed data (Osinov 2003), spontaneous channeling can be excluded with an initial $r_e = 0.5$ (rather dense). The cumulative displacements of the dam shoulder are smaller than with dry psammoid (or constant h_w), Fig. 12.5.6d, e. The pore water prevents dilation so that p_s increases, this matters more for in-plane than for anti-plane shaking. The constraint is weaker in the latter case as grain skeletons are softer for out-of-plane path reversals (Sect. 4.7). In the long run the hydraulic constraint is reduced by the diffusion of pore water.

A case with anti-plane shaking of a thin peloid layer was already outlined in Sect. 5.5. The enhanced creep or ratcheting could be captured by v-hyp- δ for lower than critical stress obliquities. A delayed collapse with shear melting and cavitation occurred with an overcritical obliquity. Apart from such critical phenomena the role of seepage can apparently be taken into account realistically for in- and anti-plane shaking of peloids.

A *composite* of psammoid and peloid zones was assumed for a case study, Fig. 12.5.7 (Gudehus et al. 2004, Libreros-Bertini 2006). A breakwater near Kobe was built upon rockfill which partly replaced soft clay, this was represented with finite elements (a). Soil parameters were chosen according to a report by Iai et al. (1998). A seismogram from the Hyogoken-Nanbu 1995 earthquake was taken as base shaking. The calculated pore pressure in the fill (b), mean skeleton pressure at the same place (c), lateral displacement at a surface point (d) and settlement of the breakwater (e) are nearly the same for in-plane and anti-plane shaking. A drainage was almost excluded during the earthquake, subsequent pore water diffusion and creep cause further displacements. The estimated asymptotic settlement of 1.5–2 m engulfs the observed one of 1.8 m.

Cases as presented above could be further investigated with the *seismodynamics* proposed in Sects. 4.6, 4.7 and 5.5. Seismodynamic equilibria were attained with submerged sand in the shakebox of Fig. 12.5.2c (Wienbroer 2010). With continued harmonic shaking the grains get unjammed so that their partial pressure gets isotropic, the void ratio gets close to the lower bound e_d and the mean pore pressure gets hydrostatic. This attractor is determined by the stationary shaking and implies a field of granular temperature T_g , observations could serve to check and quantify the balance of seismic energy by (4.6.7). The densification and the granular relaxation in the transition can at best be estimated with hyp- δ , s-hyp or h-cyc (Sect. 4.5), observations will help to validate and calibrate better theories.

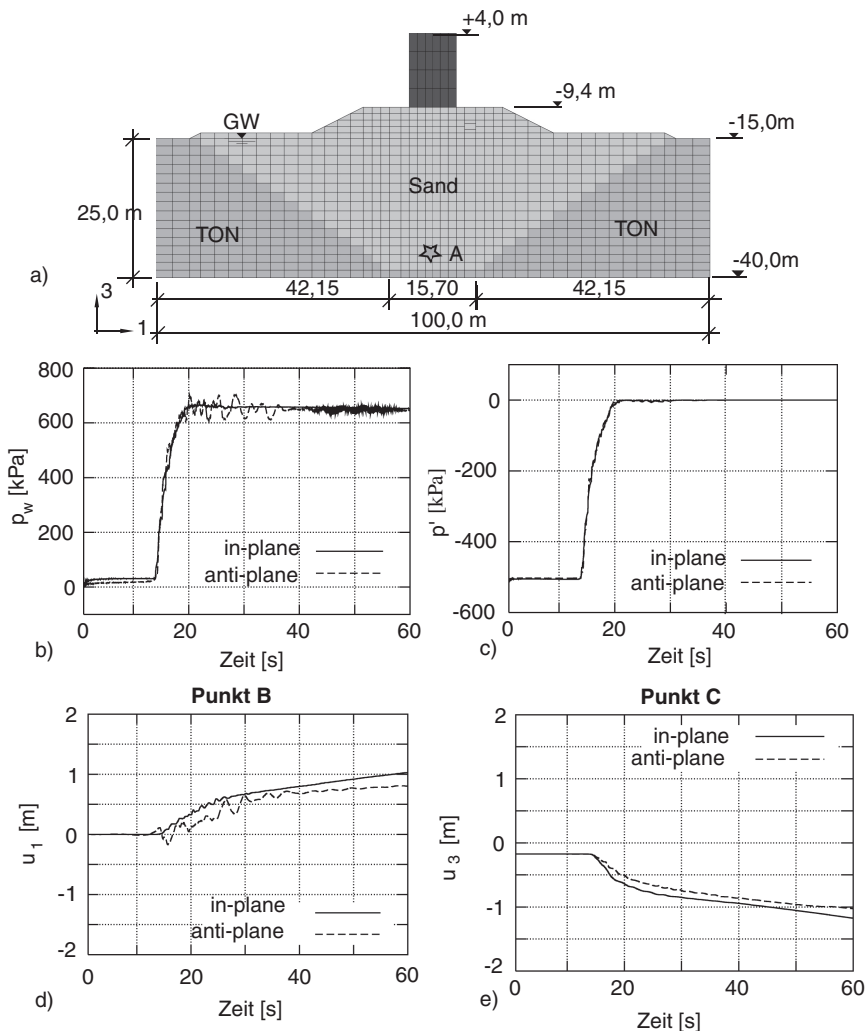


Fig. 12.5.7. Simulation of a breakwater with base shaking (Gudehus et al. 2004, Libreros-Bertini 2006): composition (a), pore pressure (b) and skeleton pressure (c) versus time for point A, horizontal displacement at the rim of fill (d) and settlement of the structure (e) versus time

Another attractor with T_g could principally be obtained by shaking the base of a granular layer with a subcritical inclination, but experiments and calculations will be difficult. In case of stationary ratcheting the grains are not unjammed, and with low T_g entropic and viscous stress fractions may be negligible. The one-dimensionality gets lost at layer rims and by critical phenomena, calculations with the models outlined in Sect. 4.5 can fail by ill-posedness. Earthquakes could produce attractors in the large with sand

which resemble thermally activated ones with peloids (Sect. 12.3), this is indicated by Fig. 12.5.6, but theories beyond hyp- δ , s-hyp and h-cyc will not easily be validated and calibrated. This holds also true for peloids with thermally *and* seismically activated viscous effects (Sect. 5.5), so Fig. 12.5.7 is no more than a promising hint.

To *sum up*, plane-parallel evolutions without structures due to base shaking can be captured by hypoplastic relations as long as critical phenomena do not dominate. Results of shake-box tests with sand are well reproduced by hyp- δ except for the formation of erosion channels after skeleton decay. Some field observations after earthquakes are fairly well reproduced with composites of psammoids and peloids. In these cases a stabilizing creep with pore water diffusion is seismically enhanced. Earth bodies at the verge of stability develop an autogeneous seismicity which indicates the onset of critical phenomena. Even without the latter the seismic mobility cannot be captured by simply assuming a temporarily heated solid.

12.6 Normal faulting

The mechanics of tectonic faulting is based on model tests with soil and on the theory of plasticity (Mandl 1988). Several kinds of fault patterns observed in situ could thus be explained, so it appears that the lithosphere is soil-like in that respect. *Normal faults* resemble shear bands in a biaxial test with horizontal stretching (Sect. 8.2). Following an article by Gudehus and Karcher (2007) it is shown in this section how evolutions of normal fault patterns can be simulated by means of hypoplasticity. As in previous sections of Chaps. 11 and 13 initial and boundary conditions have to be properly specified, now in order to get certain fault patterns. Plane-parallelity is assumed, but will be left aside at the end.

Wolf et al. (2003) obtained normal fault patterns in a model test with dry sand, Fig. 12.6.1. A dense layer was stretched by extending its laminate base via jointed parallelograms. Two out-of-plane walls were rather smooth so that nearly plane-parallel deformations were obtained. Except for the vicinity of the in-plane walls a zig-zag pattern of dilated shear bands arose by stretching (a). The free surface got wavy with steepest slopes at the outcrops of shear bands (b). The inclination of the bands against the horizontal was

$$\vartheta_n \approx 45^\circ + \varphi_p/2 \quad (12.6.1)$$

with a peak friction angle φ_p . The shear band pattern resembles swarms of normal faults (Mandl 1988). It does not arise with initially loose sand.

Nübel (2002) simulated such evolutions by means of hypoplasticity with polar quantities (cf. Sect. 8.2), Fig. 12.6.2. The rough base is extended uniformly, the in-plane walls with increasing distance are smooth and rigid. The initial relative void ratio $r_e = 0.2$ corresponds to a high density. A zig-zag



<http://www.springer.com/978-3-540-36353-8>

Physical Soil Mechanics

Gudehus, G.

2011, XIII, 840 p., Hardcover

ISBN: 978-3-540-36353-8